

A Fully Differential CMOS–MEMS DETF Oxide Resonator With $Q > 4800$ and Positive TCF

Wen-Chien Chen, *Student Member, IEEE*, Ming-Huang Li, *Student Member, IEEE*, Yu-Chia Liu, Weileun Fang, *Member, IEEE*, and Sheng-Shian Li, *Member, IEEE*

Abstract—A fully differential CMOS–MEMS double-ended tuning-fork (DETF) oxide resonator fabricated using a 0.18- μm CMOS process has been demonstrated with a Q greater than 4800 and more-than-20-dB stopband rejection at 10.4 MHz. The key to attaining such a performance attributes to the use of oxide structures with embedded metal electrodes, where SiO_2 offers a Q enhancement (at least a 3-times-higher Q) as compared to other CMOS–MEMS-based composite resonators with similar structures and vibrating modes and where flexible electrical routing facilitates fully differential configuration to suppress capacitive feedthroughs. In addition, the resonators developed in this work possess a positive temperature coefficient of frequency (TC_f) and mode-splitting capability, therefore indicating a great potential for temperature compensation and spurious-mode suppression, respectively. This technology paves a way to realize fully integrated CMOS–MEMS oscillators and filters which might benefit future single-chip transceivers for wireless communications.

Index Terms—CMOS–MEMS, double-ended tuning-fork (DETF), embedded electrode, fully differential, micromechanical resonators, oxide structure, 0.18- μm CMOS Process.

I. INTRODUCTION

VIBRATING micromechanical resonators capable of providing a high Q and zero dc power consumption have been applied into timing reference devices and oscillators in present consumer electronics [1], [2], leading to smaller size and lower cost as compared to conventional mechanical components, such as crystal [3], SAW [4], and FBAR [5]–[7] resonators. Nevertheless, the discrete nature of those off-chip micromechanical resonators still impedes the system miniaturization and circuit integration for future multiband wireless transceivers [8]. To realize MEMS resonators monolithically integrated with on-chip circuitry, in recent years, CMOS–MEMS resonator platforms based on foundry-oriented 0.35- μm 2P4M CMOS technology [9]–[11] and 0.18- μm 1P6M CMOS process [12], [13] have been developed to fabricate integrated vibrating micromechanical circuits. However, due to limited feature size and metal

stacking configuration from 0.35- μm CMOS technology [9]–[11] as well as limited transduction areas by the use of oxide-etching technique [9]–[13], CMOS–MEMS resonators mostly composed of metal-rich structures not only suffer a relatively low Q and poor thermal stability [11] but also exhibit high motional impedance R_m (i.e., low motional current) caused by either large electrode-to-resonator gap spacing or insufficient transduction area. Therefore, high-gain, large-bandwidth, and multistage sustaining circuits are necessary for integrated oscillator applications but at the expense of high power consumption. In addition, parasitic feedthrough signals often hinder the clean measurement of the desired motional current from the CMOS–MEMS resonators.

In this letter, a previously developed metal wet-etching technique capable of releasing large device areas has been successfully transferred from a 0.35- μm CMOS process [14] to a 0.18- μm technology, therefore greatly lowering the R_m due to a smaller electrode-to-resonator gap spacing and larger transduction areas. To address the unique features of the structural materials used for the CMOS–MEMS resonators in this work, SiO_2 -rich composite structures with metal electrodes embedded not only provide a higher Q than that of mere-metal [11], [12] and metal-rich [11] [13] resonators but also offer a passive temperature compensation owing to their intrinsic positive temperature coefficient of Young's modulus ($+TC_E$) [11]. To further improve the resonator performance, a vertical double-ended tuning-fork (DETF) oxide resonator with embedded metal electrodes, capable of possessing a larger transduction area A_e than its in-plane counterpart whose transduction area is often restricted by the micromachining process, was proposed to lower vibrating-energy loss at anchors for a high- Q operation. The DETF resonators in this work were experimentally verified with at least a three-times-higher Q than that of other CMOS–MEMS-based composite resonators [9]–[11], [13] with similar flexural-mode and support design. In addition, the Q of this work is also comparable to that of silicon-based DETF resonators [15]. In order to cancel the feedthrough currents, a fully differential drive/sense configuration which relies on the DETF nonconductive structure capable of applying diversified electrical settings was adopted, hence leading to a clean spectrum with more than a 14-dB improvement on the feedthrough level as compared to its single-ended counterpart. In addition, a mode-splitting capability was also realized through an elegant support design, successfully moving spurious modes away from the desired signal. As a result, the proposed CMOS–MEMS DETF oxide resonator finally demonstrated a Q of 4800, R_m of 174 k Ω , and positive TC_f with excellent signal-to-feedthrough ratio, suitable for integrated oscillator implementation in the future.

Manuscript received January 7, 2012; revised February 8, 2012; accepted February 9, 2012. Date of publication April 3, 2012; date of current version April 20, 2012. This work was supported by the National Science Council of Taiwan under Grant NSC-100-2221-E-007-033. The review of this letter was arranged by Editor E. A. Gutiérrez-D.

W.-C. Chen is with the Department of Power Mechanical Engineering, National Tsing Hua University, Hsinchu 30013, Taiwan.

M.-H. Li and Y.-C. Liu are with the Institute of Nanoengineering and Microsystems, National Tsing Hua University, Hsinchu 30013, Taiwan.

W. Fang and S.-S. Li are with the Department of Power Mechanical Engineering, National Tsing Hua University, Hsinchu 30013, Taiwan, and also with the Institute of Nanoengineering and Microsystems, National Tsing Hua University, Hsinchu 30013, Taiwan (e-mail: ssl@mx.nthu.edu.tw).

Color versions of one or more of the figures in this letter are available online at <http://ieeexplore.ieee.org>.

Digital Object Identifier 10.1109/LED.2012.2188774

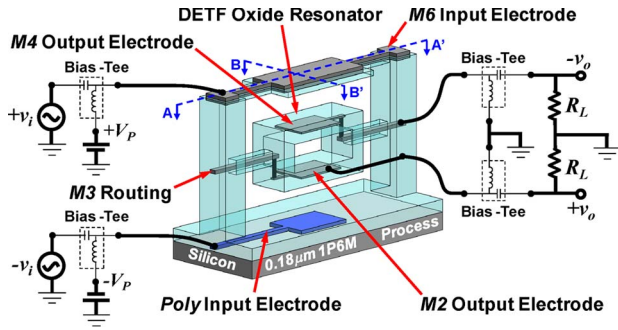


Fig. 1. Perspective-view schematic of a CMOS-MEMS DETF oxide resonator with a fully differential drive/sense configuration.

II. DIFFERENTIAL OPERATION AND MODE SPLITTING

To achieve the aforementioned performance, a vertical DETF resonator mostly made by SiO_2 with an embedded electrical routing inside to allow a fully differential operation was designed as shown in Fig. 1. To realize the fully differential operation of this work, Fig. 1 shows a drive/sense configuration for the proposed DETF oxide resonator where two embedded electrodes (M6 and Poly) serve as differentially driving ports while the other two (M4 and M2) act as differentially sensing ports. M1–M6 denote metal1–metal6, respectively, in the $0.18\text{-}\mu\text{m}$ 1P6M CMOS process where M1, M3, and M5 are used as sacrificial layers during the device release process. With an appropriate polarity of the dc-bias voltage V_P applied into the embedded electrodes of Fig. 1, the differential inputs generate specific electrostatic forces to accentuate the out-of-phase mode (cf. the simulated mode shape on the right in Fig. 5) while suppressing the in-phase mode (cf. the simulated mode shape on the left in Fig. 5). Two motional currents created by time-varying capacitances (i.e., M4-to-M6 and Poly-to-M2 capacitors) with opposite polarity then are summed together using differential sensing by which motional signals are enhanced while capacitive feedthroughs (mainly from the large bond pads) are greatly attenuated through common-mode signal cancellation. To address the spurious-mode issue from the dual-mode nature (the in-phase and out-of-phase modes) of the DETF resonator, a unique mechanical design on resonator supports (i.e., slender beams) was utilized to move the unwanted in-phase mode far away from the desired out-of-phase mode, where low-frequency out-of-plane vibrating mode merges DETF in-phase mode to substantially lower down its resonance frequency.

III. FABRICATION PROCESS AND RESULTS

To fabricate the CMOS-MEMS DETF oxide resonators, chips were manufactured using a standard TSMC $0.18\text{-}\mu\text{m}$ 1P6M CMOS process [cf. Fig. 2(a)]. Then, a metal wet etchant was utilized [14] to remove sacrificial metals [cf. Fig. 2(b)], hence providing an air-gap spacing d_{air} of $0.53\ \mu\text{m}$ and large transduction areas (e.g., $31\ \mu\text{m} \times 36\ \mu\text{m}$) to effectively lower the motional impedance of the resonators. Finally, the RIE was utilized to open bond pads [cf. Fig. 2(c)]. Fig. 3(a) shows a global SEM view for a fabricated resonator while Fig. 3(b)–(d) shows the cross-sectional images of FIB cut, including the cross-sectional view of the DETF structure, zoom-in of em-

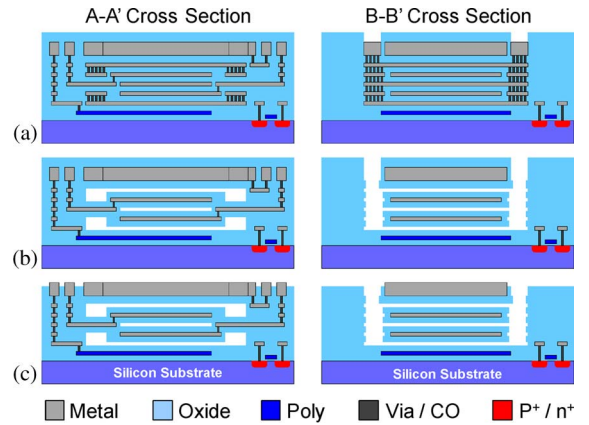


Fig. 2. Fabrication process flow. (a) After the TSMC foundry process. (b) After metal wet etching. (c) After RIE dry etching.

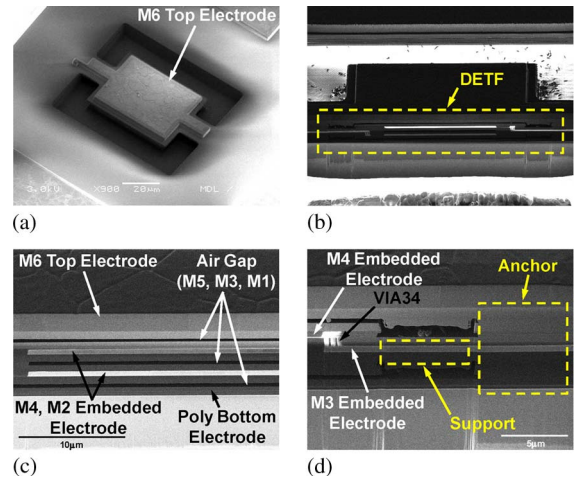


Fig. 3. SEMs including (a) global view, (b) cross-sectional view, and (c) zoom-in of the embedded metal electrodes and air gaps and (d) zoom-in of the supporting beam for a fabricated CMOS-MEMS DETF oxide resonator.

bedded metal electrodes, and zoom-in of a slender support, respectively.

IV. MEASUREMENT RESULTS

Under the test setup of Fig. 1, Fig. 4(a) presents a performance comparison between a direct two-port S_{21} (M6 for driving and Poly for sensing) and fully differential S_{dd21} measured spectra for a CMOS-MEMS DETF oxide resonator tested in vacuum, showing that the motional signal from a differential measurement is 20 dB higher than that from a direct two-port configuration while the feedthrough level is greatly improved under differential operation. Fig. 4(b) shows a differentially measured frequency response (amplitude and phase) with the highest measured Q (4805), hence indicating that the use of a SiO_2 structural material enables a high Q . The key to directly measuring Q (i.e., $f_r/\Delta f$, where f_r is the resonance frequency and Δf is the 3-dB bandwidth of the resonant peak in Fig. 4) of the proposed DETF resonator relies on the differential mode of operation where the feedthrough signals could be substantially alleviated, therefore making the direct measurement of Q possible.

To address spurious-mode issues, Fig. 5 presents a wide-span frequency characteristic using a differential setup, showing

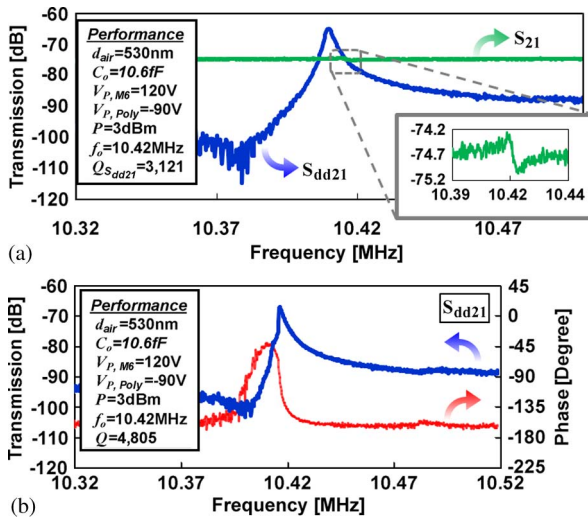


Fig. 4. S -parameter measured frequency characteristics of a fabricated CMOS–MEMS DETF oxide resonator. (a) Comparison of fully differential S_{dd21} and single-ended S_{21} frequency spectra. (b) Measured highest Q to date among the CMOS–MEMS resonators composed of metal/oxide composite structures, including S_{dd21} transmission amplitude and phase.

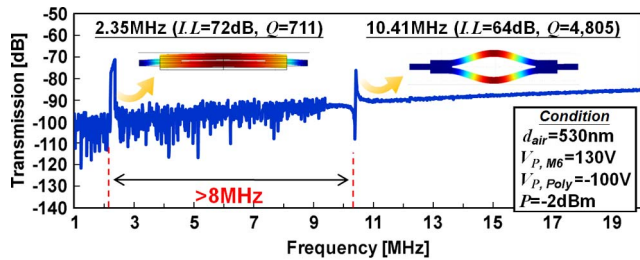


Fig. 5. Wide-span S -parameter measured frequency spectrum of a fabricated CMOS–MEMS DETF oxide resonator.

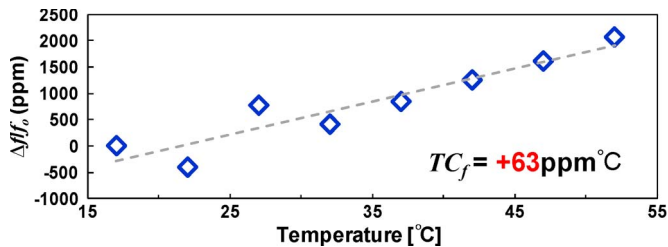


Fig. 6. Measured fractional frequency change versus temperature for a 10.42-MHz CMOS–MEMS DETF oxide resonator.

that the in-phase (unwanted) mode is more than 8 MHz away from the out-of-phase (desired) mode and verifying our mode-splitting design. Note that the in-phase mode is not completely eliminated via the use of differential transduction due to the asymmetry of the electrical configuration from the inherent mismatch of the 0.18- μm CMOS process. The transmission amplitude of the out-of-phase mode (64-dB loss) is still higher than that of the in-phase mode (72-dB loss) although the frequency response of Fig. 5 shows an opposite trend caused by the low frequency resolution of the wide-span frequency sweep. Fig. 6 finally presents frequency drift versus temperature change, showing a positive TC_f of +63 ppm/ $^{\circ}\text{C}$ for the first time among any CMOS–MEMS resonators. Note that the deviation of certain measured points away from the linear fit in Fig. 6 was mainly caused by the inferior temperature

control of the cryogenic probe station. The positive TC_f results from the extensive use of SiO_2 with positive TC_E , which is the unique feature of the process developed in this work, thus revealing that a zero TC_f by the adjustment of metal and oxide composition in such a composite resonator structure is plausible in the future.

V. CONCLUSION

This letter has reported a fully differential CMOS–MEMS DETF oxide resonator with a high Q , low motional impedance, positive temperature coefficient of frequency, and mode-splitting capability using a standard 0.18- μm foundry CMOS technology together with a simple metal-etching postprocess. The proposed technology could be easily transferred into any advanced CMOS technology nodes, such as 90-, 65-, and 45-nm processes, therefore further reducing motional impedances and dc-bias voltages of the oxide-type CMOS–MEMS resonators to facilitate integration with CMOS circuits. With such a performance and the possibility of compensation for TC_f , the results from the DETF oxide resonator developed in this work show promise to be suitable in integrated timing, oscillation, and sensor applications.

REFERENCES

- [1] *Discera DSC1001 Datasheets*, Discera Inc., San Jose, CA, 2011.
- [2] *Sitime Sit8208 Datasheets*, Sitime Inc., Sunnyvale, CA, 2011.
- [3] W. Shockley, D. R. Curran, and D. J. Koneval, "Trapped-energy modes in quartz filter crystals," *J. Acoust. Soc. Amer.*, vol. 41, no. 4B, pp. 981–993, Sep. 1967.
- [4] T. Morita, Y. Watanabe, M. Tanaka, and Y. Nakazawa, "Wideband low loss double mode saw filters," in *Proc. Ultrason. Symp.*, 1992, pp. 95–104.
- [5] R. C. Ruby, P. Bradley, Y. Oshmyansky, A. Chien, and J. D. Larson, "Thin film bulk wave acoustic resonators (FBAR) for wireless applications," in *Proc. Ultrason. Symp.*, 2001, pp. 813–821.
- [6] W. Peng, H. Yu, H. Zhang, and E. S. Kim, "Temperature-compensated film bulk acoustic resonator above 2 GHz," *IEEE Electron Device Lett.*, vol. 26, no. 6, pp. 369–371, Jun. 2005.
- [7] W. Xu, S. Choi, and J. Chae, "A contour-mode film bulk acoustic resonator of high quality factor in a liquid environment for biosensing applications," *Appl. Phys. Lett.*, vol. 96, no. 5, p. 053703, Feb. 2010.
- [8] C. T.-C. Nguyen, "MEMS technology for timing and frequency control," *IEEE Trans. Ultrason., Ferroelectr., Freq. Control*, vol. 54, no. 2, pp. 251–270, Feb. 2007.
- [9] C.-C. Lo, F. Chen, and G. K. Fedder, "Integrated HF CMOS–MEMS square-frame resonators with on-chip electronics and electrothermal narrow gap mechanism," in *Proc. Transducers Tech. Dig.*, 2005, pp. 2074–2077.
- [10] J. Verd, A. Uranga, J. Teva, J. L. Lopez, F. Torres, J. Esteve, G. Abadal, F. Perez-Murano, and N. Barniol, "Integrated CMOS–MEMS with on-chip readout electronics for high-frequency applications," *IEEE Electron Device Lett.*, vol. 27, no. 6, pp. 495–497, Jun. 2006.
- [11] W.-C. Chen, W. Fang, and S.-S. Li, "A generalized CMOS–MEMS platform for micromechanical resonators monolithically integrated with circuits," *J. Micromech. Microeng.*, vol. 21, no. 6, pp. 1–15, Jun. 2011.
- [12] J. L. Lopez, J. Verd, J. Teva, G. Murillo, J. Giner, F. Torres, A. Uranga, G. Abadal, and N. Barniol, "Integration of RF-MEMS resonators on sub-micrometric commercial CMOS technologies," *J. Micromech. Microeng.*, vol. 19, no. 1, pp. 13–22, Jan. 2009.
- [13] C.-S. Li, L.-J. Hou, and S.-S. Li, "Advanced CMOS–MEMS resonator platform," *IEEE Electron Device Lett.*, vol. 33, no. 2, pp. 272–274, Feb. 2012.
- [14] Y.-C. Liu, M.-H. Tsai, W.-C. Chen, S.-S. Li, and W. Fang, "High- Q , large-stopband-rejection integrated CMOS–MEMS oxide resonators with embedded metal electrodes," in *Proc. Transducers*, 2011, pp. 934–937.
- [15] S. Yoneoka, C. S. Roper, R. N. Candler, S. A. Chandorkar, A. B. Graham, J. Provine, R. Maboudian, R. T. Howe, and T. W. Kenny, "Characterization of encapsulated micromechanical resonators sealed and coated with polycrystalline SiC," *J. Microelectromech. Syst.*, vol. 19, no. 2, pp. 357–366, Apr. 2010.